THE NWP ACTIVITIES AT CROATIAN METEOROLOGICAL AND HYDROLOGICAL SERVICE, 2026

MARTINA ĆORKOVIĆ, SUZANA PANEŽIĆ, SARA ANĐELA PERIĆ, MARIO HRASTINSKI, ENDI KERESTURI, ENA KOŽUL RAJČIĆ, JAKOV LOZUK, ANAMARIJA MARJANOVIĆ, IRIS ODAK, INES OLROM MUIĆ, ANTONIO STANEŠIĆ, MARTINA TUDOR, IVAN VUJEC

Operational setup

Current operational model configurations:

ALADIN-HR40: Δx=4 km; 480x432x73; CY43T2; HYD dyn.; t=150 s; ALARO-1 phy.; IC: CANARI + 3DVar (3h-cycle, ENS B); 72h fcst.; LBC: IFS-3h (6-h lagged), 4 runs per day

ALADIN-HR20: Δx=2 km; 450x450x87; CY43T2; NH dyn.; DFI ini.; t=60 s; ALARO-1 phy.; 72h fcst.; IC: ALADIN-HR40; LBC: IFS 1-h (6-h lagged); 4 runs per day

Analog-based method: a statistical post-processing method that identifies analogous situations in a historical (training) period using a similarity metric, and predicts future states based on corresponding past observations; predictor weight optimization and statistical correction for rare events are also applied

Verification of operational ALADIN forecasts

The results of post processed analog-based forecast HRAN (with predictor weight optimization and correction for more extreme events included) are compared to the HR40 (for temperature variable) and HR20 (for wind speed variable) forecasts for the year 2025. Results confirm that HRAN consistently reduces overall forecast errors, primarily by lowering dispersion errors, in comparison with HR20 and HR40 (**Fig. 1**). Spatial analyses confirm that HRAN improves forecast performance across all station groups, with especially notable benefits for continental region (for wind speed) and mountainous region (for temperature).

Categorical analyses confirm that HRAN generally improves forecast performance across most of the categories. For wind speed, the improvement of HRAN in comparison with the HR20 is evident for almost all categories, especially for high wind speed events. For temperature, HR40 still shows superior results to HRAN for very low or very high temperature categories.

A paper regarding the applicability of Extremal Dependence Index (EDI) as a verification tool across a wide range of event frequencies has been submitted to Monthly Weather Review. The analysis of idealized contingency tables, as well as operational wind speed HR20 and HR40 forecasts, suggests that EDI provides a consistent and equitable assessment of forecast quality ranging from extremely rare to highly frequent events.

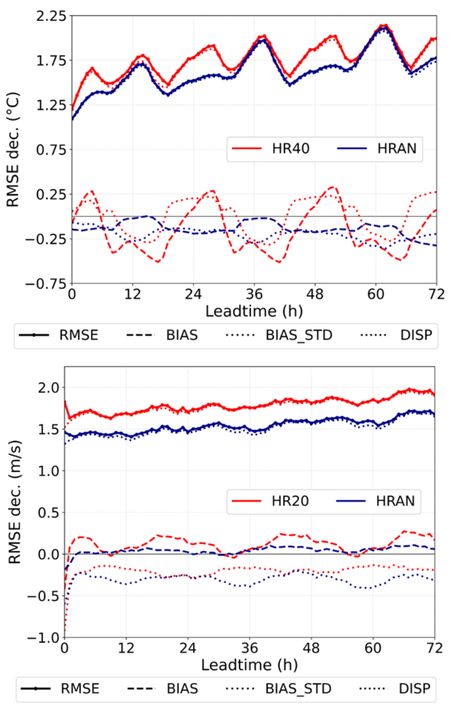

Figure 1. *RMSE decomposition for different leadtimes for temperature (top) and wind speed (bottom) forecasts. Data refer to forecasts initialized during 2025 at locations across Croatia.*

Upgrade of the national OBSOUL data used for data assimilation

Following the completion of the METMONIC (Modernisation of the National Weather Observation Network in Croatia) project, the national OBSOUL file dataset has been significantly upgraded. A total of 250 new automatic meteorological stations have been integrated into the international data exchange system. This expansion has increased the spatial coverage and improved representation of weather conditions across Croatia, including previously under-monitored areas. The METMONIC project established a modern, high-quality, and fully automated observation network. Overall infrastructure now includes 450 automatic meteorological systems, meteorological-oceanographic buoys, and advanced radar system.

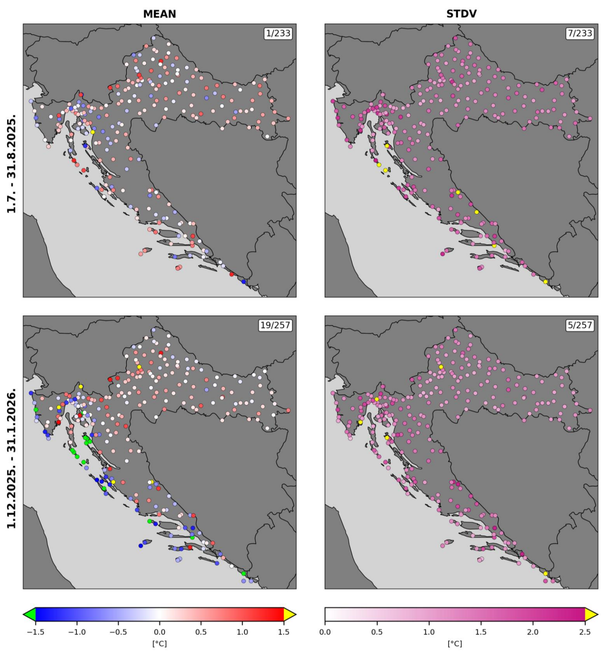

First guess departures (mean and standard deviation) were analyzed to identify large discrepancies between observations and the HR40 model background. Such discrepancies were particularly evident for mountain stations with mismatched model elevation and for stations on small islands not resolved by the 4 km model grid. Thresholds on mean and standard deviation were applied to quantify these effects (**Fig. 2**). Stations exceeding the thresholds were blacklisted and excluded from further use. The remaining stations, showing consistent statistics, were retained and used in the data assimilation system.

Figure 2. *First guess departures of the 2m temperature: mean (left) and standard deviation (right) for summer (upper) and winter (lower) periods.*

A test with an additional cloud-aware VARBC predictor is still ongoing due to its long warm up period. Even if the predictor still hasn't reached its final value after two months of cycling it can be seen that its usage stabilizes other VARBC predictors within the system (**Fig. 6**). It also reduces the bias of clear-sky and near clear-sky observations.

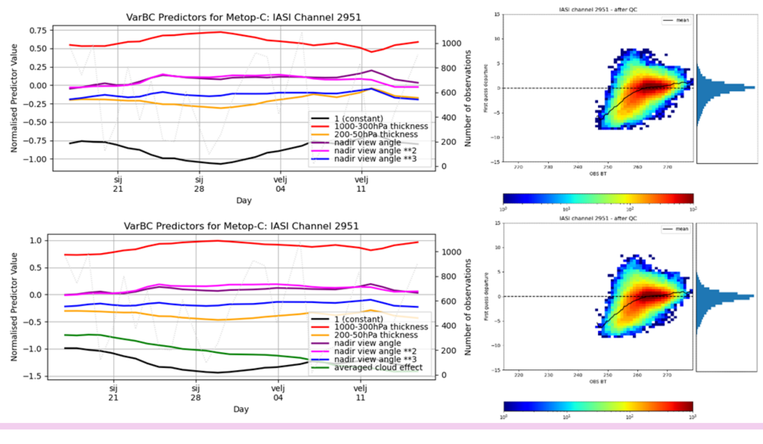

Figure 6. *Channel 2951 - METOP-C 21UTC VARBC predictor values and 2D histogram of first-guess departure depending on observed brightness temperature values; no cloud-aware predictor (upper figures) and with cloud-aware predictor (lower figures).*

All-sky assimilation of IASI data

The Metop satellites are Europe's first operational meteorological satellites in polar orbit. Each Metop satellite carries the same sophisticated suite of instruments providing fine-scale global data. One such instrument is an Infrared Atmospheric Sounding Interferometer (IASI) that measures infrared energy emitted by the earth-atmosphere system in 8461 individual spectral channels with a spatial resolution of 50 km at nadir.

Conventional clear-sky data assimilation only considers data from regions without clouds, leaving the model underrepresented in cloudy areas. In preparation for the future hyperspectral infrared sounders, the assimilation of multilayer cloud-affected infrared radiances using the all-sky approach proposed by Kozo Okamoto et al (2023) is explored. For this purpose, IASI data are used as a proxy.

The crucial part of the Okamoto approach is the observation error modeling where observation error assigned has the same size as the first guess departures standard deviation. In this sense, data is binned by the values of averaged cloud effect, defined as:

$$C_A = \frac{|B - B_{clr}| + |O - B_{clr}|}{2}$$

where B and B_{clr} are calculated simultaneously in RTTOV and represent model simulated brightness temperatures in cloudy and clear-sky scene for a given location. O is the observed brightness temperature. After that, linear fit to standard deviation values is performed, while defining minimum and maximum value that can be applied (where linear fit is a good approximation; **Fig. 3**).

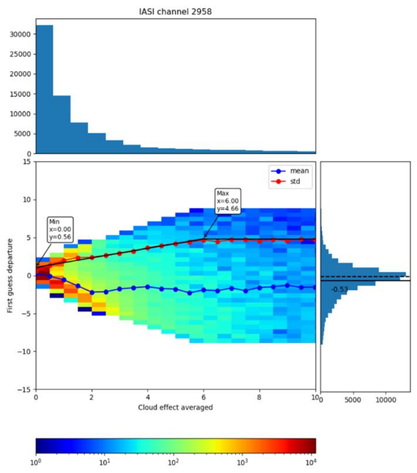

Figure 3. *2D histogram of first guess departure as a function of the averaged cloud effect; Standard deviation (red line), mean (blue line), linear fit (black line).*

The observation error is then defined as:

$$O_{err} = \frac{\sigma_{cld} - \sigma_{clr}}{C_{cld} - C_{clr}}(C_A - C_{clr})$$

where σ_{clr} and σ_{cld} are minimum and maximum values of standard deviation that can be applied and C_{clr} and C_{cld} are averaged cloud effect value at which they are assigned.

Observation error modeling was technically implemented into the CY48T3. For testing purposes 3DEnVar member of the C-LAEF (Convection-permitting Limited-Area Ensemble Forecasting) AlpeAdria system was used. Four water vapor channels were selected to be assimilated in all-sky mode: 2951, 2958, 3049 and 3105, while the rest of the channels were assimilated in the clear-sky mode.

Looking at the case of 20.01.2025., it can be seen that dynamical assignment of observation errors for all-sky channels performs as intended. Therefore, this setup can be used as the base for further development (**Fig. 4**).

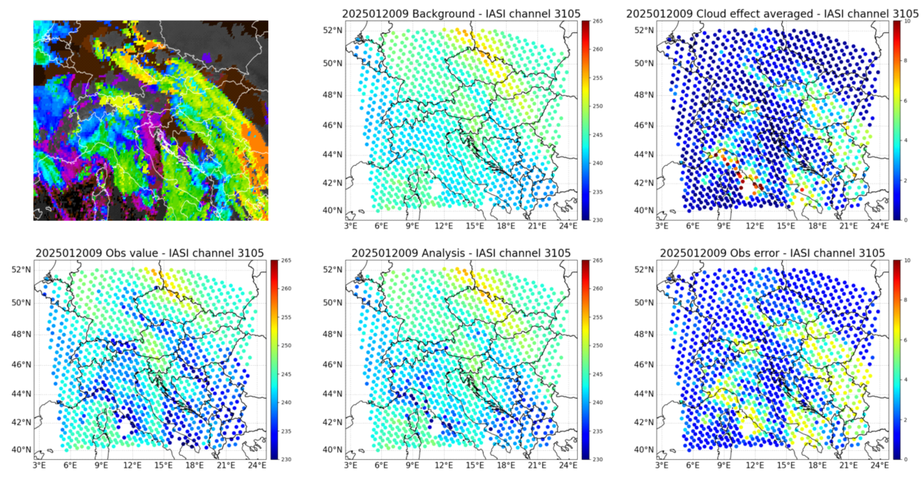

Figure 4. *Case 20.01.2025.: cloud top product (Eumetview; top left); brightness temperatures – observations (lower left), background (top middle), analysis (lower middle); averaged cloud effect (top right); assigned observation errors (lower right).*

Observations were compared to their model-equivalent values (from RTTOV) in order to identify observations that are poorly simulated by the model. Diagnostics was done using a window channel 1911 which is characterized by negligible gas absorption and a strong sensitivity to clouds (**Fig. 5**). It was shown that the model exhibits a general lack of clouds and struggles to represent very cold cloud tops, typically associated with high ice clouds. Therefore, observations with brightness temperatures below 240 K should be rejected.

Additional tests were performed by rejecting strongly-affected data (averaged cloud effect > 5.0 K) and opaque clouds (transmittance (tau) > 0.01). In order to evaluate the impact of different all-sky components in the assimilation of IASI data, ODB content was explored. In particular, their influence on other types of assimilated observations, such as radiosounding and AIREP data, was assessed. These observations provide valuable information across the full vertical profile of the atmosphere and are therefore well suited for quantifying the impact of all-sky IASI assimilation on the model background state. It was shown that appropriate quality control keeps a larger number of radiosounding and AIREP data with improved or neutral impact for all variables. However, if observations with brightness temperatures < 240K are not rejected, the negative increments meant for the upper atmosphere can be incorrectly projected to lower levels, which can degrade near-surface temperature and humidity. Additional tests are needed to find the exact mechanism for near-surface degradation.

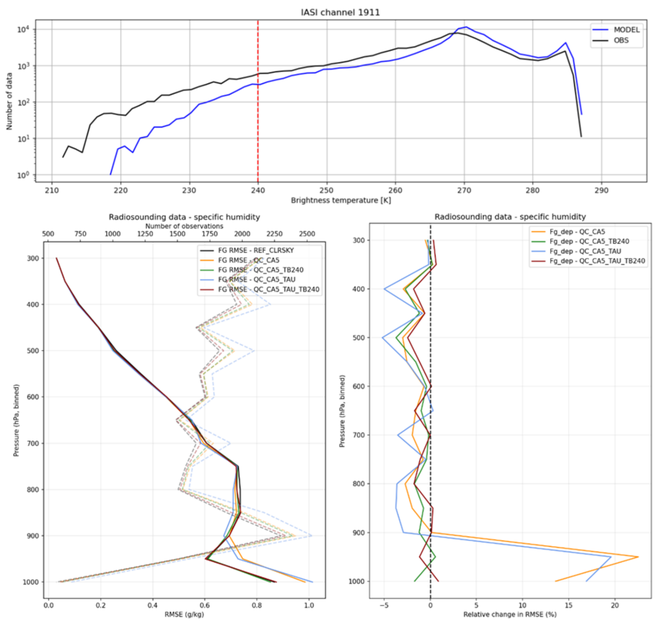

Figure 5. *Channel 1911 diagnostics - number of observed and model-equivalent data per brightness temperature; Impact on radiosounding data - RMSE of specific humidity and its relative change depending on a clear-sky reference (CA5 - rejection of data with averaged cloud effect > 5; TAU - rejection of data with transmittance > 0.01; TB240 - rejection of data with brightness temperature < 240 K).*